PHYSICAL REVIEW D VOLUME 27, NUMBER 1 1 JANUARY 1983

Quark model for baryons based on quantum chromodynamics

J. Carlson, J. Kogut, and V. R. Pandharipande
Department of Physics, University of Illinois at Urbana-Champaign, 1110 W. Green Street, Urbana, Illinois 61801
(Received 16 July 1982)

SU(3) flux-tube dynamics and asymptotic freedom are incorporated into a semirelativistic quark model of baryons and mesons. Good agreement with the energy levels of spin-averaged multiplets of mesons and baryons is obtained using conventional values for the strong-interaction coupling constant α_s, the string tension $\sqrt{\sigma}$, and the constituent quark mass m. We calculate meson energy levels with angular momentum $L=0$, 1, 2, 3, and 4 and baryon levels with $L=0$, 1, and 2 to within 3% of their experimental values. Baryon radial excitations are also considered and the Roper resonance is calculated with $\sim 5\%$ error. The three-body wave equation for the baryons is solved approximately using variational Monte Carlo methods which have been developed previously for nuclear-physics problems.

I. INTRODUCTION

In the past decade quantum chromodynamics[1] (QCD) has emerged as the most promising theory of hadrons. In the nonrelativistic, i.e., static-source limit the basic SU(3) flux-tube picture leads to a Coulomb + linear potential between $q\bar{q}$ pairs. Such a potential has been used in a nonrelativistic Schrödinger equation to calculate the spectrum of charmonium[2,3] and $b\bar{b}$ states.[3] The color-magnetic interactions due to one-gluon exchange have also been used to study the hyperfine splittings within multiplets of light mesons[4] and baryons.[4,5]

The aim of this paper is to abstract current ideas of quark-gluon dynamics from QCD into a semirelativistic Hamiltonian for $q\bar{q}$ and qqq systems. This Hamiltonian contains an adiabatic potential obtained by minimizing the energy in the gauge fields for fixed quark positions, and relativistic kinetic energies for the quarks. It is shown that such a Hamiltonian is justified for QED in $(1+1)$ dimensions, where the potential between the charges is linear.

In the limit of massive quarks our semirelativistic Hamiltonian for $q\bar{q}$ systems becomes identical to that used in Ref. 3 for charmonium and $b\bar{b}$ studies. However, it is meant to be useful for the study of light mesons, and it does explain quite accurately their spectra associated with orbital excitations.

Our model for baryons is more novel. In a color-singlet qqq system, each quark acts as a source of one flux tube. For SU(3) gauge fields, the flux tubes can merge at a single point P between the quarks. Minimizing the energy in the flux tubes determines the location P and the qqq potential. The baryon potential is, therefore, intimately related to the SU(3) color group. We find that the potential energy of three quarks forming a baryon can be expressed as a sum of three pair potentials and a relatively weaker three-body potential. The pair potential in baryons is exactly half the potential between $q\bar{q}$, and the three-body potential depends only on the tension in SU(3) flux tubes. Thus, from the point of view of many-body theory, a unified model for studying baryon and meson spectra is proposed. The present study is limited to the baryon spectrum associated with orbital and radial excitations, and thus complements the studies[4,5] of the hyperfine splittings. Our spectrum calculations are in good agreement with experiment.

This paper is organized into four sections. In Sec. II, we discuss SU(3) flux tubes in the context of lattice formulations of QCD. We motivate our semirelativistic potential model by considering the fully relativistic Schwinger model (QED in $1+1$ dimensions). In Sec. III we describe the variational method used to calculate eigenvalues of the semirelativistic two- and three-body Hamiltonians. Results and discussion appear in Sec. IV.

II. THE MODEL HAMILTONIANS

Recent numerical work[6,7] on lattice QCD and its continuum limit support the naive physical picture and properties of gluon dynamics which follows. The Hamiltonian for SU(3) gluons interacting among themselves, modeled on a spatial cubic lattice of spacing a is

$$H=\frac{g^2}{2a}\left[\sum_{\text{links}} E^2(l)-\frac{2}{g^4}\sum_{\text{plaquettes}}(\text{tr}UUUU+\text{H.c.})\right] . \tag{2.1}$$

The $E^2(l)$ measures the color-electric flux along link l, and $UUUU$ indicates the product of color-rotation matrices taken around a closed square (plaquette) as shown in Fig. 1. Equation (2.1) is a locally gauge-invariant, lattice-regulated form of the ordinary energy in the Yang-Mills field, and g is a coupling constant which can be identified with the conventional quantity in the continuum limit in which the lattice spacing a tends to zero. The basic commutation relation satisfied by the $E^\alpha(l)$ and $U_{ij}(l)$ follows from their geometric meaning as the $\alpha=1,8$ generators of the color rotations, and $i,j=1,3$ color-rotation matrices, respectively,

$$[E^\alpha(l),U_{ij}(l')]=\tfrac{1}{2}[\lambda^\alpha U(l)]_{ij}\delta_{ll'} . \tag{2.2}$$

Here λ^α are SU(3) matrices. Let $|0\rangle$ be the "vacuum" state with no color-electric flux:

$$E^\alpha(l)\,|0\rangle=0 . \tag{2.3}$$

The state $U_{ij}(l)\,|0\rangle$ has one unit of electric flux on link l,

$$\begin{aligned}E^2(l)U_{ij}(l)\,|0\rangle&=(\tfrac{1}{4}\lambda^\alpha\lambda^\alpha U)_{ij}(l)\,|0\rangle\\&=\tfrac{4}{3}U_{ij}\,|0\rangle ,\end{aligned} \tag{2.4}$$

as can be verified with Eq. (2.2). Thus $U_{ij}(l)$ matrices create additional flux along link l.

The last fundamental ingredient in the theory is the requirement of local gauge invariance. This means that only states corresponding to operators whose color indices at every lattice point are contracted into color singlets are physically realized. For example, an isolated $U_{ij}(l)$ is not locally gauge invariant. Since it has two free color indices it transforms as $(\bar{3},3)$. However, ordered products of U matrices on closed paths through the lattice are acceptable.

The states

$$U_{ij}(l_1)U_{jk}(l_2)\cdots U_{mi}(l_n)\,|0\rangle , \tag{2.5}$$

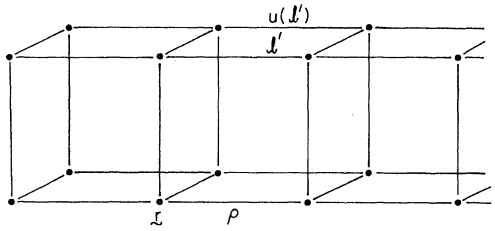

FIG. 1. Three-dimensional cubic lattice with sites r, links l, and color-rotation matrices $U(l)$ assigned to links.

where links $l_1,l_2,\ldots,l_n$ form a closed loop, are gauge invariant. (By convention a sum over repeated color indices is implied.) These states describe loops of color-electric flux.

If quarks are incorporated into the scheme as color sources, the flux tubes can originate and terminate on the quark. Let $\psi_i^\dagger(\vec{r})$ create a quark on site $\vec{r}$, and $\psi_m(\vec{r}')$ create an antiquark on site $\vec{r}'$. Then a locally gauge-invariant operator to create a $q\bar{q}$ state would be

$$\psi_i^\dagger(\vec{r})U_{ij}(l_1)U_{jk}(l_2)\cdots U_{lm}(l_n)\psi_m(\vec{r}') , \tag{2.6}$$

where the links $l_1,l_2\ldots l_n$ form a path from $\vec{r}$ and $\vec{r}'$, and the repeated color indices are summed. Physically the string of U matrices carries the unit of flux emanating from the quark and terminating on the antiquark. These states are used to describe the mesons.

To estimate the force, i.e., the dependence of energy on $|\vec{r}-\vec{r}'|$, we must determine the path of the U matrices in the lowest-energy state. It is believed that the strong-coupling limit $g^2\gg1$ of the lattice theory describes many of the relevant features of the long-distance behavior of Yang-Mills fields. It is trivial to calculate the path of the U matrices in this limiting case in which the magnetic-fluctuation term (tr $UUUU$) in Eq. (2.1) can be neglected. The Hamiltonian then reduces to $\sum E^2(l)$, and the energy of the state (2.6) is

$$\frac{g^2}{2a}\times\frac{4}{3}(\text{number of links})=\frac{2g^2}{3a^2}(\text{path length}) . \tag{2.7}$$

The minimum path length is simply the distance $|\vec{r}-\vec{r}'|$, and this gives the familiar confining potential

$$V(\vec{r}-\vec{r}')=\sqrt{\sigma}\,|\vec{r}-\vec{r}'| , \quad \sqrt{\sigma}=2g^2/3a^2 . \tag{2.8}$$

Numerical studies[6,7] of lattice gauge theory suggest that a linear confining potential also occurs in the continuum limit. Therefore, it is sensible to use it in quark models of mesons as has been done by many authors.[2,3,8]

The potential at small distances can be calculated perturbatively using asymptotic freedom of the theory. It is

$$V(\vec{r}-\vec{r}')=-\frac{4\alpha_s}{3\,|\vec{r}-\vec{r}'|} , \quad |\vec{r}-\vec{r}'|<1/\sqrt{\sigma} , \tag{2.9}$$

where $\alpha_s=g^2/4\pi$ is the strong-interaction fine-structure constant. It has a weak spatial dependence

given by asymptotic freedom[9]:

$$\alpha_s = -\frac{2\pi}{11\ln(\Lambda\,|\,\vec{r}''-\vec{r}'\,|\,)} . \tag{2.10}$$

These long- and short-range parts can be easily incorporated into a single $q\bar{q}$ potential

$$V_{q\bar{q}}(\vec{r}-\vec{r}') = -\frac{4}{3}\frac{\alpha_s}{|\,\vec{r}-\vec{r}'\,|} + \sqrt{\sigma}\,|\,\vec{r}-\vec{r}'\,| \tag{2.11}$$

which has been used to study meson spectra of heavy[3] $(c,b,\ldots)$ and light[8] $(u,d,s\ldots)$ quarks. Although the potential (2.11) captures much of the physics of gluons, it is certainly not complete. For example, very general arguments concerning the dynamics of long flux tubes indicate that there are (universal) power-law corrections to Eq. (2.8) of the type

$$V(\vec{r}-\vec{r}') = \sqrt{\sigma}\,|\,\vec{r}-\vec{r}'\,| - \frac{\pi}{12\,|\,\vec{r}-\vec{r}'\,|} + \cdots , \quad |\,\vec{r}-\vec{r}'\,| \gg 1/\sqrt{\sigma} \tag{2.12}$$

induced by long-wavelength transverse fluctuations of the tube.[10] In practice[3] some of these effects are taken into account approximately by fitting α_s and $\sqrt{\sigma}$ to the data, rather than carrying out a first-principles calculation. In such fits the weak spatial dependence of α_s [Eq. (2.10)] may be neglected.

Even with the potential Eq. (2.11) in hand it is not obvious how to incorporate it into a potential-model calculation of the meson spectrum. Various questions arise: Should V be treated as a Lorentz vector or scalar quantity? Is it restricted to only nonrelativistic $q\bar{q}$ systems? What about retardation effects, quantum fluctuations such as virtual and real pair production, etc? To gain some perspective on these questions consider the simplest soluble model of quark confinement and flux tubes, the Schwinger model (quantum electrodynamics in $1+1$ dimensions). Its Lagrangian is

$$L = -\tfrac{1}{4}F_{\mu\nu}F^{\mu\nu} + \bar{\psi}(i\partial\!\!\!/ - gA\!\!\!/ - m)\psi , \tag{2.13}$$

where

$$F_{\mu\nu} = \partial_\mu A_\nu - \partial_\nu A_\mu . \tag{2.14}$$

The Hamiltonian of this theory is particularly revealing in the Coulomb gauge where Gauss's law,

$$\partial_1{}^2 A_0 = -g{:}\psi^\dagger\psi{:} \equiv g j_0 \tag{2.15}$$

becomes an equation of constraint. Then an elementary exercise yields

$$H = \int dx\,\bar{\psi}(i\gamma_1\partial_1 + m)\psi - \tfrac{1}{4}g^2\int dx\,dy\,j_0(x)j_0(y)\,|\,x-y\,| . \tag{2.16}$$

The linear confinement mechanism is clear in the second term. The theory confines simply because electric flux is always in straight tubes in $1+1$ dimensions. Because of this, the Schwinger model is often used as a theoretical laboratory for some of the long-distance features of gluon dynamics in $3+1$ dimensions. Note also that Eq. (2.16) describes fully relativistic, causal dynamics since it follows by canonical methods from Eq. (2.13).

Next consider Eq. (2.16) restricted to the $q\bar{q}$ subspace. Denote a two-particle state $|\,p,q\,\rangle$ where p is the momentum of the quark and q is the momentum of the antiquark. Following Ref. 11, consider the reduced (center-of-mass) Hamiltonian,

$$\langle q',p'\,|\,H\,|\,p,-p\rangle = \delta(p'+q')\langle p'\,|\,H^R\,|\,p\,\rangle . \tag{2.17}$$

The fermion field operator

$$\psi(x) = \frac{1}{\sqrt{2\pi}}\int dp[\,a(p)u(p)e^{ipx} + b^\dagger(p)v(p)e^{-ipx}] , \tag{2.18}$$

where

$$\{a(p),a^\dagger(p')\} = \delta(p-p') , \tag{2.19}$$

$$(\alpha p + \beta m)u = Eu , \tag{2.20}$$

$$E = (p^2+m^2)^{1/2} , \quad u^\dagger(p)u(p) = 1 , \tag{2.21}$$

and similarly for the positron operators and spinors. Substituting Eq. (2.18) into Eq. (2.16) and evaluating Eq. (2.17) gives,

$$H^R = 2(p^2+m^2)^{1/2} + \tfrac{1}{2}g^2\,|\,x\,| \tag{2.22}$$

in the approximation where field theoretic fluctuations such as pair production are ignored. It is interesting that Eq. (2.22) is fully relativistic and that the linear confining potential appears here without being obscured by retardation or velocity-dependent effects. This simplicity, of course, relies on the kinematics of $1+1$ dimensions, but we shall use it as a guidepost in our $3+1$ dimension potential-model work. In particular, we shall treat the quark kinetic energy fully relativistically—this is necessary for light-quark spectroscopy—and use the potential energy given by the strong-coupling behavior at long distances and asymptotic freedom at short distances.

The major aim of this work is the construction and analysis of a quark model for *baryons* which incorporates features of gluon dynamics of QCD. Therefore, consider the $g^2 \gg 1$ behavior of flux tubes in the presence of *three* heavy quarks. Each quark is the source of one unit of electric flux. The lowest-energy state of the three quarks will have the least amount of flux consistent with local gauge in-

variance. There are two distinct flux configurations depending on the relative positions of the quarks. Consider the quarks in positions $\vec{r}_1$, $\vec{r}_2$, and $\vec{r}_3$ as shown in Fig. 2. Suppose that none of the interior angles of the triangle whose vertices are $\vec{r}_1$, $\vec{r}_2$, and $\vec{r}_3$ are greater than 120°. Then the flux tubes from each quark will meet in the interior at positions $\vec{r}_4$, and the total energy in the configuration is

$$V(\vec{r}_1\vec{r}_2\vec{r}_3)=\frac{2g^2}{3a^2}(\,|\vec{r}_1-\vec{r}_4|+|\vec{r}_2-\vec{r}_4| + |\vec{r}_3-\vec{r}_4|\,) . \tag{2.23}$$

It is crucial that in SU(3) gauge theory the vertex at $\vec{r}_4$ can be constructed in a locally gauge-invariant fashion. The operator which creates the state at strong coupling is

$$\psi_i^\dagger(\vec{r}_1)\psi_j^\dagger(\vec{r}_2)\psi_k^\dagger(\vec{r}_3) \times\left[\prod_{p_1}U\right]_{ir}\left[\prod_{p_2}U\right]_{js}\left[\prod_{p_3}U\right]_{kt}\epsilon_{rst} , \tag{2.24}$$

where p_i indicates the path from $\vec{r}_i$ to $\vec{r}_4$ and ϵ_{rst} is the usual antisymmetric tensor. Recall that in SU(3) $3\otimes 3\otimes 3=1\otimes 8\otimes 8\otimes 10$, and the singlet is the antisymmetric product of the three objects each transforming as a $\vec{3}$. Finally, the position $\vec{r}_4$ is determined by the condition that it minimize the static energy,

$$\vec{\nabla}_4 V=0 \tag{2.25}$$

or

$$\sum_i \hat{r}_{i4}=0 , \tag{2.26}$$

where $\hat{r}_{i4}=(\vec{r}_i-\vec{r}_4)/|\vec{r}_i-\vec{r}_4|$. As shown in the figure, the angles that the flux tubes make with one another are 120° *independent* of the $\vec{r}_i$ themselves.

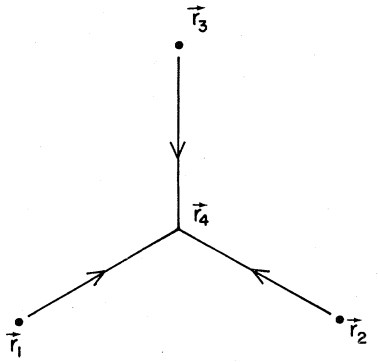

FIG. 2. The flux-tube configuration in a three-quark state at strong coupling, when none of the interior angles of the triangle $\vec{r}_1\vec{r}_2\vec{r}_3$ are greater than 120°.

It is clear, however, that if one of the interior angles i of the triangle $\vec{r}_1\vec{r}_2\vec{r}_3$ is greater than 120° Eq. (2.26) cannot be satisfied and the flux tube from the vertex i will collapse to a point. Then the flux configuration will consist of two linear segments as shown in Fig. 3.

For completeness we eliminate $\vec{r}_4$ from Eq. (2.23). An exercise in trigonometry gives for the flux configuration of Fig. 2

$$|\vec{r}_i-\vec{r}_4|\equiv r_{i4}=(C^2-r_{jk}^2)/S , \quad (i,j,k \text{ cyclic}) , \tag{2.27}$$

where

$$C^2=\tfrac{1}{2}\xi+(\tfrac{1}{3}\eta-\tfrac{1}{12}\xi^2)^{1/2} , \tag{2.28}$$

$$S^2=3C^2-\xi , \tag{2.29}$$

$$\xi=r_{12}^2+r_{23}^2+r_{31}^2 , \tag{2.30}$$

$$\eta=r_{12}^2r_{23}^2+r_{23}^2r_{31}^2+r_{31}^2r_{12}^2 . \tag{2.31}$$

For the flux configuration in Fig. 3 we note that $\vec{r}_4=\vec{r}_i$.

It is instructive to decompose the total potential energy (2.23) of the *qqq* system in the long-range (LR) region into "two-body" and "three-body" interactions as follows:

$$V_{\rm LR}(\vec{r}_1,\vec{r}_2,\vec{r}_3) =\sum_{i<j}\tfrac{1}{2}\sqrt{\sigma}r_{ij}+\sqrt{\sigma}\left[\sum_i r_{i4}-\tfrac{1}{2}\sum_{i<j}r_{ij}\right] . \tag{2.32}$$

This decomposition is meaningful because the three-body term is relatively small compared to the sum of two-body terms. The ratio

$$\left[\sum_i r_{i4}-\tfrac{1}{2}\sum_{i<j}r_{ij}\right]\Big/\left[\tfrac{1}{2}\sum_{i<j}r_{ij}\right]$$

is zero when the quarks are in a line, and it ap-

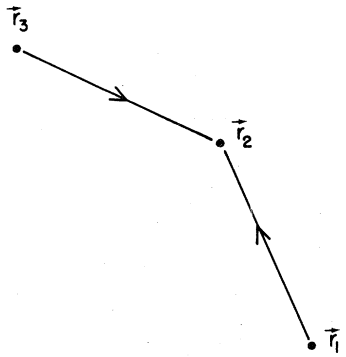

FIG. 3. The flux-tube configuration in a three-quark state when the angle at $\vec{r}_2$ is greater than 120°.

proaches zero when one of the quarks is pulled far away from the other two. It has its maximum value of 0.154 when the quarks form an equilateral triangle.

The short-range (SR) interaction is simply the two-body color-Coulomb force

$$V_{\rm SR}(\vec{r}_1,\vec{r}_2,\vec{r}_3)=-\tfrac{1}{2}\sum_{i<j}\frac{4\alpha_s}{3r_{ij}} . \tag{2.33}$$

The factor of $\frac{1}{2}$ is due to the one-gluon-exchange potential between a qq pair in a qqq color singlet being half as strong as that between a $q\bar{q}$ pair in a $q\bar{q}$ singlet.[10] Thus if we define $v(r)$ to be the two-body potential in a $q\bar{q}$ state as given by Eq. (2.11) the potential energy of the qqq system is given by

$$V(\vec{r}_1,\vec{r}_2,\vec{r}_3)=\tfrac{1}{2}\sum_{i<j}v(r_{ij}) +\sqrt{\sigma}\left[\sum_i r_{i4}-\tfrac{1}{2}\sum_{i<j}r_{ij}\right] . \tag{2.34}$$

In the next section this potential will be added to the relativistic kinetic energy $\sum_i(p_i^2+m^2)^{1/2}$ to obtain the Hamiltonian for baryons.

The factor of $\frac{1}{2}$ relating the short-range part of the two-body $q\bar{q}$ and qq interactions is well known,[4] and the energy differences between spin multiplets can be used to test its validity. The same factor $\frac{1}{2}$ also relates the long-range $q\bar{q}$ and qq interactions. Phenomenologically it is important because (i) it guarantees that baryon Regge trajectories have the same slope as the meson trajectories and (ii) it allows the spacings in low-energy meson and baryon spectra to be explained with the same string tension $\sqrt{\sigma}$. An optimist can interpret this success in explaining the hadron spectra as an evidence for flux tubes as suggested by QCD.

There are several ways one might imagine improving and generalizing the considerations of this section. Spin effects might be accounted for by including the color-hyperfine terms from the short-range one-gluon-exchange graphs.[4] Considerable work has been done on this subject with some good results.[5] Multiquark states and glueballs could also be studied in the flux-tube framework suggested here. In fact, we are engaged in some exploratory work in these directions.

III. VARIATIONAL CALCULATIONS

The meson and baryon spectra, in the simplest model which neglects the coupling of baryon states to baryon + meson, and of meson states to multimeson states, are given by the eigenvalues of the Schrödinger equation

$$H\psi=E\psi , \tag{3.1}$$

where for nonstrange mesons we have

$$H=\sum_{i=1,2}(p_i^2+m^2)^{1/2}+v(r_{ij})+E_0^M \tag{3.2}$$

and for nonstrange baryons

$$H=\sum_{i=1,3}(p_i^2+m^2)^{1/2}+V(\vec{r}_1,\vec{r}_2,\vec{r}_3)+E_0^B . \tag{3.3}$$

The $v(r)$ and $V(\vec{r}_1,\vec{r}_2,\vec{r}_3)$ are given by Eqs. (2.11) and (2.34), respectively, and m is the mass of u,d quarks. The E_0^M and E_0^B are constants to be determined from data. We refer to Hamiltonians (3.2) and (3.3) as semirelativistic (SR) models.

We also discuss solutions of the corresponding nonrelativistic (NR) Hamiltonians:

$$H=\sum_{i=1,2}\frac{p_i^2}{2m}+v(r_{ij})+E_0^M , \tag{3.4}$$

$$H=\sum_{i=1,3}\frac{p_i^2}{2m}+V(\vec{r}_1,\vec{r}_2,\vec{r}_3)+E_0^B . \tag{3.5}$$

The Schrödinger equation can be trivially solved for only the Hamiltonian (3.4). The eigenvalues of the other Hamiltonians (3.2), (3.3), and (3.5) are calculated with the variational method.

The variational wave functions for the $q\bar{q}$ and qqq states are taken to be

$$\psi_{l,q\bar{q}}(\vec{r}_{12})=f(r_{12})\phi_l(\vec{r}_{12}) , \tag{3.6}$$

$$\psi_{n,qqq}(\vec{r}_{12},\vec{r}_{23})=F_{123}\left[\prod_{i<j}f(r_{ij})\phi_n(\vec{r}_{12},\vec{r}_{13})\right] . \tag{3.7}$$

The $f(r)$ are parametrized functions of r, while F_{123} is a function of r_{12}, r_{13}, and r_{31}. These functions are varied to minimize the energy of the state. The ϕ's are constructed so that the ψ has appropriate quantum numbers. The $\phi_l(\vec{r}_{12})$ of $q\bar{q}$ states are taken as

$$\phi_l(\vec{r}_{12})=r_{12}{}^lY_l^M(\theta_{12}\phi_{12}) ; \tag{3.8}$$

these generate states of angular momentum l with no radial excitations.

The qqq states are classified by the total angular momentum L, parity π, and symmetry under spatial permutations. The ground state is a 0^+ spatially symmetric state, to be multiplied with a [symmetric SU(6)] $\otimes$ [antisymmetric color] wave function to obtain a fully antisymmetric wave function. Similarly, spatially mixed symmetric (antisymmetric) states are to be used with mixed symmetric (antisymmetric) SU(6) states to obtain nonstrange and strange baryons.

A mixed-symmetry state may be classified as a ρ- or λ-type state obeying the following relations under permutations:

$$P_{23}\psi_\lambda=\psi_\lambda\ ,\quad P_{23}\psi_\rho=-\psi_\rho\ , \tag{3.9}$$

$$P_{12}\psi_\lambda=\frac{\sqrt{3}}{2}\psi_\rho-\tfrac{1}{2}\psi_\lambda\ ,$$
$$P_{12}\psi_\rho=\tfrac{1}{2}\psi_\rho+\frac{\sqrt{3}}{2}\psi_\lambda\ , \tag{3.10}$$

$$P_{13}\psi_\lambda=-\frac{\sqrt{3}}{2}\psi_\rho-\tfrac{1}{2}\psi_\lambda\ ,$$
$$P_{13}\psi_\rho=\tfrac{1}{2}\psi_\rho-\frac{\sqrt{3}}{2}\psi_\lambda\ . \tag{3.11}$$

Examples of $L^\pi=1^-$ states of ρ and λ type are

$$\psi_{1^-\rho}=\frac{1}{\sqrt{2}}(z_3-z_2)\ , \tag{3.12}$$

$$\psi_{1^-\lambda}=\frac{1}{\sqrt{6}}(z_2+z_3-2z_1)\ . \tag{3.13}$$

The ρ and λ states having the same quantum numbers are of course degenerate.

The ϕ_n's for the lowest seven qqq states are given in Table I. It should be noted that these states are translationally invariant, i.e., $P=0$ states of the baryon, and consequently the ψ_n's also have total momentum $P=0$. All states other than the two symmetric 0^+ states are orthogonal to each other by construction, while the parameter α in the ϕ of the excited 0^+S(Roper resonance) state is adjusted to make the ψ_{0+S}(ground) and ψ_{0+S}(Roper) orthogonal.

We first discuss the parametrization of $f(r)$ and F_{123} for the NR three-body Hamiltonian (3.5). The $f(r)$ in this case is taken as

$$-\ln f(r)=W(r)\lambda_1 r+[1-W(r)]\lambda_{1.5}r^{1.5}\ , \tag{3.14}$$

$$W(r)=\frac{1+\exp(-r_0/a)}{1+\exp[(r-r_0)/a]}\ , \tag{3.15}$$

with λ_1, $\lambda_{1.5}$, a, and r_0 as variational parameters.

TABLE I. The ϕ functions of baryon states. The $\rho_\pm$, ρ_0, $\lambda_\pm$, and λ_0 are spherical-tensor components of the vectors $\vec{\rho}=(\vec{r}_2-\vec{r}_3)/\sqrt{2}$ and $\vec{\lambda}=(\vec{r}_2+\vec{r}_3-2\vec{r}_1)$.

L	π	Symmetry	ϕ
0	+	S	1
1	−	M	ρ_0
0	+	S	$1-\alpha(\rho^2+\lambda^2)$
0	+	M	$\vec{\rho}\cdot\vec{\lambda}$
2	+	S	$3(\rho_0^2+\lambda_0^2)-(\rho^2+\lambda^2)$
2	+	M	$3\rho_0\lambda_0-\vec{\rho}\cdot\vec{\lambda}$
1	+	A	$\rho_-\lambda_+-\rho_+\lambda_-$

This $f(r)$ gives a nonrelativistic Coulomb-type wave function at small r, and that appropriate to a linear potential at large r. The λ_1 is fixed so that the singular $(2\alpha_s/3r_{ij})\psi$ term in the Schrödinger equation is canceled by the $\hbar^2/m\,(\nabla^2 f_{ij}/f_{ij})\psi$ term. This gives

$$\gamma_1=+\frac{2}{3}\alpha_s\frac{mc}{2\hbar}\ . \tag{3.16}$$

The value of the parameter $\lambda_{1.5}$ can be estimated by examining the wave function in the limit $r_1\sim r_2$ and $r_{31}\sim r_{32}\gg 1/\sqrt{\sigma}$. In the limit $r_{13}\sim r_{32}=r\to\infty$ it can be seen[12] that the $f^2(r)$ is the solution of a two-body Schrödinger equation with reduced mass $\mu=\frac{2}{3}m$, and potential $\sqrt{\sigma}r$. Thus

$$\frac{3\hbar^2}{4m}\nabla^2 f^2(r)\sim\sqrt{\sigma}rf^2(r)\ ,\quad \lim r\to\infty \tag{3.17}$$

gives $\lambda_{1.5}$ as

$$\lambda_{1.5}\sim\left[\frac{4\sqrt{\sigma}m}{27\hbar^2}\right]^{1/2}\ . \tag{3.18}$$

The F_{123} is meant to take into account the influence of the three-body interaction in the qqq potential energy [Eq. (2.34)] on the wave function. Since this interaction is rather weak we use the F_{123} suggested by perturbation theory[13]:

$$F_{123}=\left[1-\beta\sqrt{\sigma}\left[\sum_i r_{14}-\tfrac{1}{2}\sum_{i<j}r_{ij}\right]\right]\ , \tag{3.19}$$

and vary β to minimize the energy. The F_{123} correlation simply reduces the magnitude of ψ in the regions where the three-body potential is repulsive.

The potential energy $V(qqq)$ is a smooth function of $\vec{r}_1,\vec{r}_2,\vec{r}_3$, and so rather accurate solutions of this NR three-body problem are obtained with these simple variational wave functions. For example, the calculated expectation value $\langle(H_{\rm NR})^2\rangle$ is close to $(\langle H_{\rm NR}\rangle)^2$ and the quantity

$$\frac{\langle(H_{\rm NR})^2\rangle^{1/2}-\langle H_{\rm HR}\rangle}{\langle H_{\rm NR}\rangle} \tag{3.20}$$

is ~ 0.001 for all states. The highest value for the above ratio is 0.0013 for the 0^+S(Roper) state. The estimated error in the variational energy of the 0^+S(ground) state,

$$\Delta E(0^+S\text{ ground})=\frac{\langle(H_{\rm NR})^2\rangle_G-(\langle H_{\rm NR}\rangle_G)^2}{\langle H_{\rm NR}\rangle_R-\langle H_{\rm NR}\rangle_G}\ , \tag{3.21}$$

where $\langle\ \rangle_G$ and $\langle\ \rangle_R$ denote expectation values for the ground and Roper states, is ~ 4 MeV. The expression (3.21) generally overestimates the error in

the variational energies.

We basically assume that the eigenfunctions of the SR Hamiltonians are similar to those of the NR Hamiltonians. Variational calculations with the SR qqq Hamiltonian (3.3) are carried out with a slightly more general $f(r)$ given by

$$-\ln f(r)=W(r)(\gamma_1 r+\gamma_2 r^2) +[1-W(r)]\gamma_{1.5} r^{1.5} , \quad (3.22)$$

and F_{123} given by Eq. (3.19). In test calculations on two-body systems it was noticed that the equilibrium value of γ_1 is close to the NR estimate (3.16) and hence γ_1 is kept fixed at that value, and the other parameters $\gamma_{1.5}$, a, r_0, and γ_2 are varied to minimize the energy. The γ_2 has little effect on the calculated eigenvalues.

It is well known[14] that the wave function of the relativistic hydrogen atom is singular at the origin. The variational $f(r)$ for the SR $q\bar{q}$ problem is parametrized to allow for such a singularity:

$$f(r)=r^{\delta}\exp\{-W(r)\gamma_1 r -[1-W(r)]\gamma_{1.5} r^{1.5}\} . \quad (3.23)$$

The γ_1 is kept fixed at its NR value:

$$\gamma_1=\frac{4}{3}\alpha_s\frac{m}{2}\frac{1}{(1+l)} , \quad (3.24)$$

and δ, $\gamma_{1.5}$, r_o, and a are varied to minimize the energy. From the relativistic-hydrogen-atom wave function we expect δ in the $l=0$ state to be

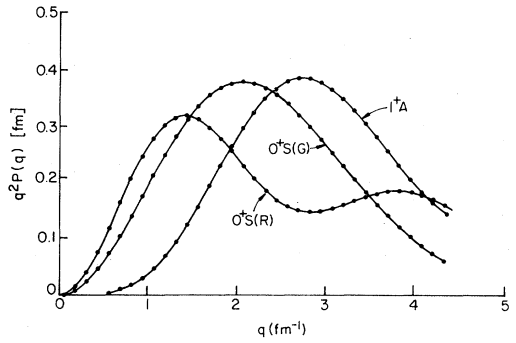

FIG. 4. The momentum distribution in three-quark states.

$$\delta\sim\left[1-\left[\frac{4\alpha_s}{3}\right]^2\right]^{1/2}-1 \sim -0.134 . \quad (3.25)$$

The equilibrium value of δ in $l=0$ state is found to be ~ -0.2. The r^{δ} in $f(r)$ has very little effect on the energy; the $l=0$ state energy increases by only ~ 5 MeV on setting $\delta=0$. Hence the r^{δ} factor is omitted in the calculations of $l>0$ mesons. In principle the $f(r)$ [Eq. (3.22)] used in qqq calculations should also have a r^{δ} factor, but the effective fine-structure constant there is $2\alpha_s/3\sim 0.25$, which yields an estimated value $\delta\sim -0.03$ that is too small to influence variational energies.

In NR qqq calculations the expectation values of

TABLE II. Details of SR kinetic-energy calculation. All the momentum-space results are with $p_m=4.417$ fm^{-1}.

	$\langle k_i^2\rangle$ (fm^{-2})	$\langle k_i^4\rangle$ (fm^{-4})	$\sum_i\langle(m^2+p_i^2)^{1/2}\rangle$ (GeV)
0^+S ground			
Coordinate space	7.77	119.7	
Momentum space $p<p_m$	5.96	54.0	1.671
Momentum space and tail	7.77	133.1	1.794
Parametrized $P(p)$	7.77	119.7	1.803
0^+S Roper			
Coordinate space	11.02	256.9	
Momentum space $p<p_m$	6.19	67.5	1.668
Momentum space and tail	11.02	282.1	1.998
Parametrized $P(r)$	11.02	256.9	2.034
1^+A			
Coordinate space	11.21	195.2	
Momentum space $p<p_m$	8.45	91.2	1.920
Momentum space and tail	11.21	205.8	2.103
Parametrized $P(r)$	11.21	195.2	2.109

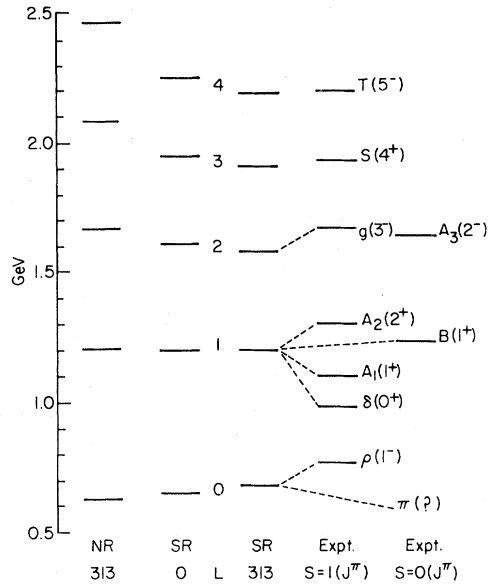

FIG. 5. The calculated meson spectra are compared with the experimental data (Ref. 17).

the potential energy $\langle V\rangle$, of kinetic energy $\langle T\rangle$, and those of V^2, ∇^4, and $\nabla^2 V+V\nabla^2$ operators are calculated with the Monte Carlo method.[15] From these we trivially obtain the $\langle H\rangle$ and $\langle H^2\rangle$. In SR calculations the expectation value

$$\langle T\rangle \equiv \left\langle \sum_i (m^2+p_i^2)^{1/2} \right\rangle$$

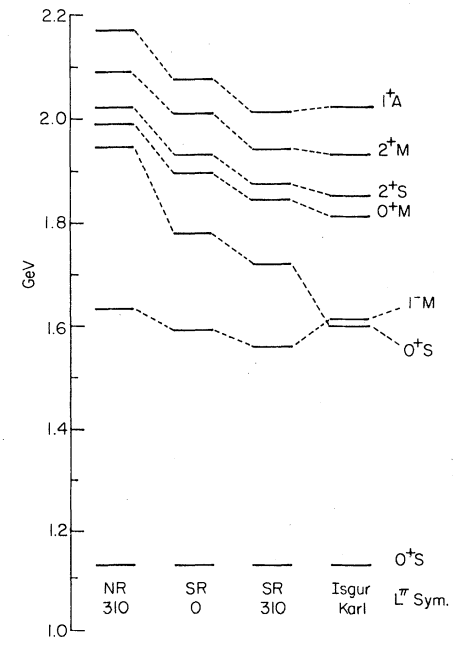

FIG. 6. The calculated baryon spectra are compared with that of Isgur and Karl.

TABLE III. The values of E_0^M and E_0^B in GeV.

Model	m	E_0^M	E_0^B
NR	313	0.372	0.676
SR	0	0.547	0.940
SR	313	0.735	1.265

is calculated in momentum space. It is relatively easy to take Fourier transforms of the two-body $q\bar{q}$ wave function. Those of the three-body wave function are calculated as follows.

Let $p^2P_i(p)$ be the probability of quark i to have momentum of magnitude p:

$$\int P_i(p)p^2dp=1\ , \tag{3.26}$$

$$\langle (m^2+p_i^2)^{1/2}\rangle = \int P_i(p)(m^2+p^2)^{1/2}p^2dp\ . \tag{3.27}$$

The $P_i(p)$ is given by

$$P_i(p)=\frac{1}{N}\int d^3r_i d^3r_i' d^3r_j d^3r_k \frac{\sin(p\mid \vec{r}_i-\vec{r}_i'\mid)}{p\mid \vec{r}_i-\vec{r}_i'\mid} \times\psi^*(\vec{r}_i'\vec{r}_j\vec{r}_k)\psi(\vec{r}_i\vec{r}_j\vec{r}_k)\ , \tag{3.28}$$

where N is determined from the normalization (3.26). The integral (3.28) is evaluated by the Monte Carlo method up to a certain maximum value p_m beyond which accurate numerical calculations become difficult. The calculated momentum distributions are shown in Fig. 4 for 0^+S ground and Roper states, and the 1^+A state of the three-quark system with $m=313$ MeV.

The $p<p_m$ states give $\sim 90\%$ of the SR kinetic energy (Table II), however they account for a much smaller fraction of the expectation values $\langle p_i^2\rangle$ and $\langle p_i^4\rangle$ obtained from $\langle -\nabla^2\rangle$ and $\langle \nabla^4\rangle$ in coordinate space. The $P_i(p>p_m)$ is approximated by an exponential ae^{-bp}. The parameter a is determined from continuity of $P_i(p)$ at p_m, while b is obtained from the $\langle p_i^2\rangle$ calculated in coordinate space. Comparison of $\langle k^4\rangle$ calculated from the $P_i(b)$ and $\langle \nabla^4\rangle$, given in Table II suggests that this treatment

TABLE IV. Parameters of meson wave functions in fm.

L	γ_1	$\gamma_{1.5}$	r_0	a	δ
0	0.3965	2.1	0.15	0.05	−0.2
1	0.1982	2.2	0.15	0.1	0.0
2	0.1322	2.1	0.25	0.2	0.0
3	0.0991	2.2	0.3	0.3	0.0
4	0.0793	2.2	0.3	0.3	0.0

TABLE V. Properties of meson wave functions in fm.

L	$\langle k^2 \rangle$	$\langle k^4 \rangle$	$\langle r^2 \rangle^{1/2}$
0	7.93	a	0.29
1	8.97	132.6	0.43
2	11.16	180.9	0.53
3	14.56	281.8	0.60
4	16.48	347.5	0.69

[a]Divergent.

of the tail of $P_i(p)$ is adequate, though not exact.

The above calculation of $\langle (m^2+p_i^2)^{1/2} \rangle$ is rather time consuming, and a much simpler method is used for minimizing $\langle H \rangle$ in SR calculations. We assume a functional form for the $\sum_i P_i(p)$,

$$\sum_i P_i(p) = \frac{3}{N}(xp)^y \exp(-xp) , \tag{3.29}$$

and calculate x and y from the $\langle \nabla^2 \rangle$ and $\langle \nabla^4 \rangle$. The $\sum_i \langle (m^2+p_i^2) \rangle$ is estimated using this functional form. As can be seen from Table II this simpler calculation is quite accurate, and we test its accuracy at the end of the variational calculation by the detailed calculation of $\sum_i \langle (m^2+p_i^2) \rangle$ for the optimum wave functions.

IV. RESULTS

All the results reported in this section are obtained with the values

$$\tfrac{4}{3}\alpha_s = 0.5 , \tag{4.1}$$

$$\sqrt{\sigma} = 1 \text{ GeV/fm} , \tag{4.2}$$

that are consistent with the values 0.52 and 0.93 GeV/fm used to fit the spectrum of charmonium.[3] The calculated spectra are shown in Figs. 5 and 6. The constant E_0^M in the meson Hamiltonian is fixed so that the calculated energy of the $L=1$ mesons is 1203 MeV which corresponds to the center of mass of the $J^\pi = 0^+$, 1^+, and 2^+ $\delta(980)$, $A_1(1100)$, and $A_2(1310)$ mesons. These mesons are believed to have $L=1$ and spin $S=1$. The $L=1$, $S=0$, $J^\pi = 1^+$ meson is believed to be the $B(1235)$, thus the $\vec{\sigma}_1 \cdot \vec{\sigma}_2$ interaction in $L=1$ mesons appears to be negligible. The E_0^B is fixed so that the 0^+S qqq ground state is at 1.135 GeV as determined by Isgur and Karl.[5] The values obtained for E_0^M and E_0^B in various models are given in Table III. At present these constants cannot be computed from basic principles.

TABLE VI. Properties of baryon wave functions in fm.

State	$\left\langle \sum_i k_i^2 \right\rangle$	$\left\langle \sum_i k_i^4 \right\rangle$	$\langle r^2 \rangle^{1/2}$
$0^+S(G)$	23.4	359	0.33
1^-M	28.8	491	0.48
$0^+S(R)$	33.1	771	0.66
0^+M	33.3	640	0.65
2^+S	32.3	591	0.67
2^+M	33.2	593	0.65
1^+A	33.6	586	0.64

TABLE VII. Details of the meson energies in GeV.

L	$\langle (m^2+p^2)^{1/2} \rangle$	$\langle -4\alpha_s/3r \rangle$	$\langle \sqrt{\sigma} r \rangle$
0	1.18	−0.27	0.52
1	1.29	−0.15	0.80
2	1.41	−0.11	1.02
3	1.59	−0.09	1.15
4	1.68	−0.08	1.33

We have ignored the quark spins in our calculations. The $\vec{\sigma}_1 \cdot \vec{\sigma}_2$ and $\vec{L} \cdot \vec{S}$ forces are believed to be of short range,[4] and the observed energies of $L=2$ mesons are indeed not too sensitive to the value of total spin. Hence, it is meaningful to compare the energies of $L>2$ mesons with experiment. Figure 5 reveals that the calculated meson spectra for the SR model with $m=313$ are within a few percent of the experiment, and a detailed study of hyperfine splittings is necessary to determine the deviations from experiment. The energy of the $L=0$ state of this model is 0.68 GeV. It is likely that the $\vec{\sigma}_1 \cdot \vec{\sigma}_2$ interaction will push the $L=0$, $S=1$ ρ-meson state to approximately the correct energy. The $L=0$, $S=0$ state may not come as low as the π meson.

Isgur and Karl[5] have analyzed the spectra of baryons starting from a Hamiltonian:

$$H = H_0 + H_{\text{hyp}} , \tag{4.3}$$

where H_0 contains the kinetic and spin-independent forces, while H_{hyp} contains spin-spin and tensor terms. The eigenvalues of H_0 are taken as free parameters to be determined from the experimental masses, and H_{hyp} is treated as a perturbation. The present work complements that of Isgur and Karl; we calculate the eigenfunctions and eigenvalues of H_0. Hence it is meaningful to compare our results with the eigenvalues of H_0 deduced from the experimental masses in Ref. 5. Figure 6 shows that the SR model with $m=313$ MeV is indeed in good agreement with the data.

The calculated energies of the 1^-M, 0^+M, 2^+S, 2^+M, and 1^+A states are within 3% of those of Isgur and Karl, but the 0^+S(Roper) is too high by 120 MeV, or 7.5%. It should be noted here that Isgur and Karl obtain the N^* Roper resonance at 1405

TABLE VIII. Details of the baryon energies in GeV.

State	$\langle(m^2+p^2)^{1/2}$	$\langle -2\alpha_s/3r_{ij}\rangle$	$\langle\frac{1}{2}\sqrt{\sigma}r_{ij}\rangle$	$\langle\sqrt{\sigma}(r_{i4}-\frac{1}{2}r_{ij})\rangle$
$0^+S(G)$	1.80	−0.34	0.86	0.08
1^-M	1.96	−0.27	1.04	0.10
$0^+S(R)$	2.01	−0.30	1.17	0.11
0^+M	2.08	−0.25	1.20	0.08
2^+S	2.06	−0.24	1.22	0.10
2^+M	2.09	−0.23	1.22	0.12
1^+A	2.11	−0.21	1.23	0.15

MeV, i.e., about 65 MeV too low compared with the experimental 1470 MeV. Thus the unperturbed energy of the 0^+S(Roper) state could be ~ 65 MeV above that indicated by Isgur and Karl. Second, we note that the $J^\pi=\frac{7}{2}^+$ states $\Delta(1950)$ and $N(1990)$ give clear indications for the unperturbed energies of the 2^+S and 2^+M states, but those of the 0^+M and 1^+A are not that uniquely determined from the data.

The spectra of SR Hamiltonians are not too sensitive to the assumed value of u,d quark mass in the relativistic kinetic energy. The level spacings generally reduce by $\sim 15\%$ as we go from NR $m=313$ MeV, SR $m=0$ to SR $m=313$ MeV models. However, the 0^+S Roper resonance state is particularly sensitive to the form of kinetic energy. We have not attempted to fit the meson masses or Isgur and Karl energies by carefully varying α_s, $\sqrt{\sigma}$, and m. It may be possible to obtain a little better agreement with a few percentage smaller value of $\sqrt{\sigma}$.

The equilibrium values of the parameters for the meson wave function are given in Table IV. For the baryons, the parameters in the wave function were essentially identical in all states, within the accuracy of the method. Even in the nonrelativistic case, where our results should be most accurate, the parameters change very little for the different states. For the $m=313$ MeV semirelativistic case, the parameters are

$$\gamma_2=0.637\ \text{fm}^{-2}\ ,\quad \gamma_{1.5}=1.40\ \text{fm}^{-1.5}\ ,$$
$$r_0=0.12\ \text{fm}\ ,\quad a=0.12\ \text{fm}\ ,$$
$$\beta=0.25\ \text{GeV}^{-1}\ .$$

The k^2, k^4, and rms radii are given in Tables V and VI and the expectation values of the kinetic, color-Coulomb, linear, and three-body potentials are given in Tables VII and VIII. These tables report results obtained with the SR $m=313$ MeV model.

We learn from these tables that the hadronic states in this model are relatively small and contain rather energetic constituents. In particular, the proton has a rms radius of $\simeq\frac{1}{3}$ fm and each quark in it has an average kinetic energy of approximately 600 MeV. Studies of the large-transverse-momentum distributions of the fragments of hadronic collisions suggest quark kinetic energies of this order.[17] The small rms size of the proton suggested here is consistent with other quark models but is considerably smaller than values favored by phenomenologists. It has been suggested in the literature[18] that quark calculations of $\langle r^2\rangle^{1/2}$ give the "core size" of the proton. There is in addition the pion cloud surrounding the proton which is not accounted for in our model and may be responsible for the large proton-size estimates deduced from peripheral-scattering processes.

Note added in proof. Cutkosky and Hendrick[19] have considered the long-range interaction given by Eq. (2.23) in baryons. Stringlike solutions of the bag model[20] give meson Hamiltonians similar to Eq. (3.2).

ACKNOWLEDGMENT

This work was supported by the National Science Foundation under Grants Nos. NSF PHY81-21399 and NSF PHY82-01948.

[1]J. Kogut and L. Susskind, Phys. Rev. D 11, 395 (1975).
[2]E. Eichten, K. Gottfried, T. Kinoshita, J. Kogut, K. D. Lane, and T. M. Yan, Phys. Rev. Lett. 34, 369 (1975).
[3]E. Eichten, K. Gottfried, T. Kinoshita, K. D. Lane, and T. M. Yan, Phys. Rev. D 21, 203 (1980).
[4]A. De Rújula, Howard Georgi, and S. L. Glashow, Phys. Rev. D 12, 147 (1975).
[5]Nathan Isgur and Gabriel Karl, Phys. Rev. D 18, 4186 (1978); 19, 2653 (1979); 20, 1191 (1979).
[6]J. Kogut, R. B. Pearson, and J. Shigemitsu, Phys. Rev. Lett. 43, 484 (1979).
[7]M. Creutz, Phys. Rev. D 21, 2308 (1980).
[8]J. F. Gunion and R. S. Willey, Phys. Rev. D 12, 174 (1975); J. F. Gunion and L. F. Li, *ibid.* 12, 3583 (1975).
[9]W. Fischler, Nucl. Phys. B129, 157 (1977).
[10]M. Lüscher, Nucl. Phys. B180, 317 (1981).
[11]R. P. Feynman, M. Kislinger, and F. Ravndal, Phys. Rev. D 3, 2706 (1971).

[12]J. Lomnitz Adler and V. R. Pandharipande, Nucl. Phys. A342, 404 (1980).
[13]J. Carlson and V. R. Pandharipande, Nucl. Phys. A371, 301 (1981).
[14]J. D. Bjorken and S. D. Drell, *Relativistic Quantum Mechanics* (McGraw-Hill, New York, 1964).
[15]J. Lomnitz Adler, V. R. Pandharipande, and R. A. Smith, Nucl. Phys. A361, 399 (1981).
[16]R. P. Feynman, R. D. Field, and G. C. Fox, Phys. Rev. D 18, 3320 (1978).
[17]Particle Data Group, Rev. Mod. Phys. 52, S1 (1980).
[18]G. E. Brown and M. Rho, Phys. Lett. 82B, 197 (1979); G. E. Brown, Nucl. Phys. A374, 63c (1982).
[19]R. E. Cutkosky and R. E. Hendrick, Phys. Rev. D 16, 786 (1977); 16, 793 (1977).
[20]K. Johnson and C. B. Thorm, Phys. Rev. D 7, 1934 (1976).